

# RSC Advances



This is an *Accepted Manuscript*, which has been through the Royal Society of Chemistry peer review process and has been accepted for publication.

*Accepted Manuscripts* are published online shortly after acceptance, before technical editing, formatting and proof reading. Using this free service, authors can make their results available to the community, in citable form, before we publish the edited article. This *Accepted Manuscript* will be replaced by the edited, formatted and paginated article as soon as this is available.

You can find more information about *Accepted Manuscripts* in the [Information for Authors](#).

Please note that technical editing may introduce minor changes to the text and/or graphics, which may alter content. The journal's standard [Terms & Conditions](#) and the [Ethical guidelines](#) still apply. In no event shall the Royal Society of Chemistry be held responsible for any errors or omissions in this *Accepted Manuscript* or any consequences arising from the use of any information it contains.

Cite this: DOI: 10.1039/c0xx00000x

www.rsc.org/xxxxxx

ARTICLE TYPE

# Ferroelectric-gate thin-film transistors with $\text{Bi}_{3.15}\text{Nd}_{0.85}\text{Ti}_3\text{O}_{12}$ gate insulators on $\text{LaNiO}_3$ -buffered Si substrates

H. J. Song,<sup>a,b</sup> T. Ding,<sup>a,b</sup> X. L. Zhong,<sup>\*a,b</sup> J. B. Wang,<sup>\*a,b</sup> B. Li,<sup>a,b</sup> Y. Zhang,<sup>a</sup> C. B. Tan,<sup>a,b</sup> and Y. C. Zhou<sup>a</sup>

Received (in XXX, XXX) Xth XXXXXXXXX 20XX, Accepted Xth XXXXXXXXX 20XX

DOI: 10.1039/b000000x

Ferroelectric-gate thin-film transistors (FGTs) with a stacked oxide structure of  $\text{ZnO}/\text{Bi}_{3.15}\text{Nd}_{0.85}\text{Ti}_3\text{O}_{12}$  (BNT)/ $\text{LaNiO}_3$  (LNO) on Si substrates have been prepared and characterized. The FGTs devices show good electrical properties, such as large “on” current of  $2.5 \times 10^{-4}$  A and low threshold voltage of 1.1 V. These are mainly attributed to the coupling enhancement of the gate electric field to the channel layer due to *a*-axis preferential orientation of BNT ferroelectric-gate insulator thin films obtained by using the LNO buffer layer and the relatively good interface properties. The results suggest that  $\text{ZnO}/\text{BNT}/\text{LNO}/\text{Si}$  structures are well suited for thin-film transistors for future nonvolatile memory applications.

## Introduction

Ferroelectric-gate thin-film transistors (FGTs) have attracted much attention due to their simple device structure, non-destructive readout operation, low power consumption and high endurance.<sup>1-6</sup> The various types of FGTs composed of different stacked structures have been investigated.<sup>7-13</sup> Nevertheless, the gate insulators of most of these thin-film transistors are epitaxial ferroelectric thin films grown on some special substrates (e.g.,  $\text{SrTiO}_3$ ). The expensive substrates and the incompatibility with the well-established Si technology will hinder the progress of the FGTs applications. Thus, developing Si-based thin-film transistors with high-quality ferroelectric thin films as gate insulators is significant for promoting the FGTs applications. Up until now, few researches have reported the FGTs deposited directly on Si substrates.

Ferroelectric bismuth-layer perovskite films such as  $\text{SrBi}_2\text{Ta}_2\text{O}_9$  (SBT) and lanthanide-doped  $\text{Bi}_4\text{Ti}_3\text{O}_{12}$  (BIT) are recognized as promising materials for FGTs applications due to their high fatigue resistance and large dielectric constant.<sup>14</sup> As we know, while ferroelectric film has a strongly anisotropic polarization and dielectric properties. For example, the

polarization of BIT is as large as  $50 \mu\text{C}/\text{cm}^2$  along *a*-axis but rather small as  $4 \mu\text{C}/\text{cm}^2$  along *c*-axis and the dielectric constant of the *a*-axis-oriented film is much larger than that of the *c*-axis-oriented film.<sup>15, 16</sup> In fact, unfortunately the films of these materials are easily grown with the *c*-axis perpendicular to the film plane (i.e., the *c*-axis orientation) because of the highly anisotropic structures,<sup>17</sup> which influences the properties of corresponding devices. Therefore, in order to achieve bismuth-layered perovskite film FGTs with good performance, *a*-axis-oriented film with a high polarization and dielectric constant is essential. Using an appropriate buffer layer with specific orientation is a good way to grow non *c*-axis-oriented bismuth-layered perovskite films on Si substrates. For example, by using (110)-oriented  $\text{SrRuO}_3$  (SRO) and (100)-oriented  $\text{Y}_2\text{O}_3$ -stabilized  $\text{ZrO}_2$  (YSZ) buffer layers, Lee *et al.*<sup>17, 18</sup> have fabricated the *a*-axis-oriented  $\text{Bi}_{3.25}\text{La}_{0.75}\text{Ti}_3\text{O}_{12}$  (BLT) films on Si (100)

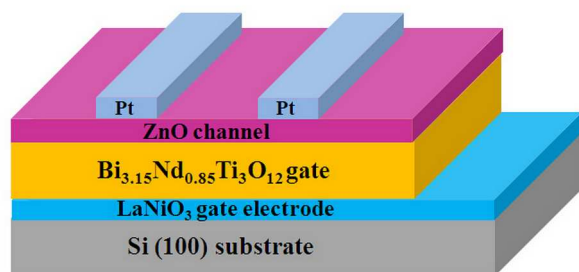


Fig. 1 Schematic illustration of the  $\text{ZnO}/\text{BNT}/\text{LNO}/\text{Si}$  FGTs

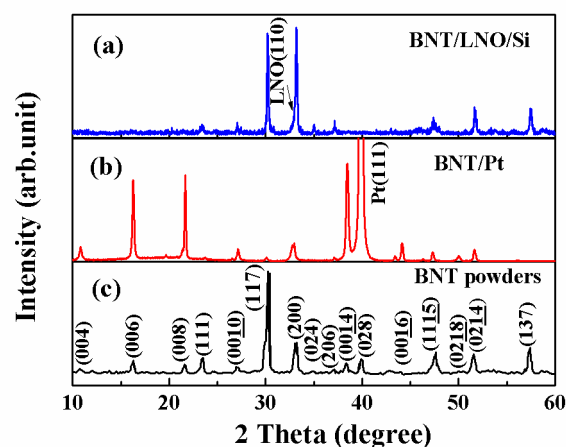


Fig. 2 The XRD patterns of (a) the BNT thin films deposited on LNO electrodes, (b) the BNT thin films deposited on Pt electrodes, and (c) the BNT powders.

Cite this: DOI: 10.1039/c0xx00000x

www.rsc.org/xxxxxx

ARTICLE TYPE

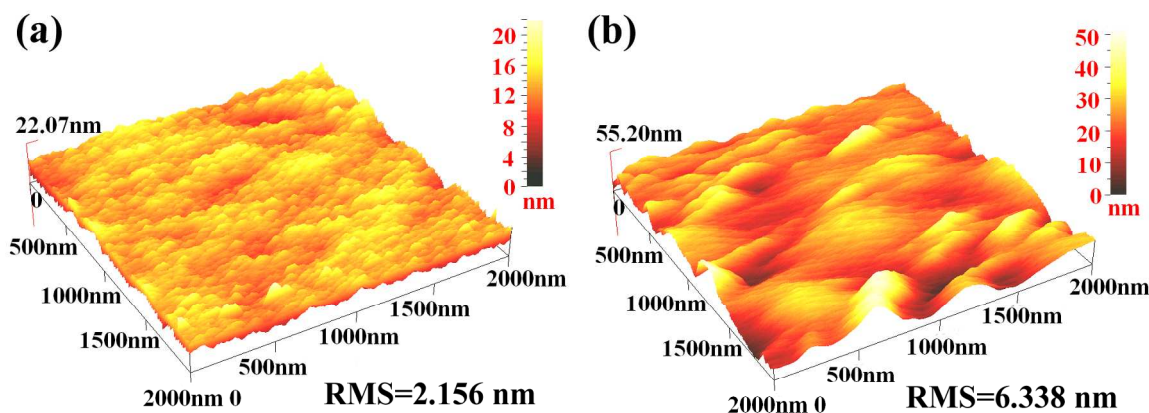


Fig. 3 AFM 3D images of the BNT films deposited on (a) LNO and (b) Pt electrodes.

substrates. Perovskite  $\text{LaNiO}_3$  (LNO) not only has same chemistry structure and close crystal constant with SRO, but also has lower cost than SRO. Furthermore, LNO can act as a good electrode layer due to its low resistivity and good metallic conductivity.<sup>10, 19</sup> Therefore, in this paper we use LNO as the buffer layer and  $\text{Bi}_{3.15}\text{Nd}_{0.85}\text{Ti}_3\text{O}_{12}$  (BNT) as ferroelectric-gate insulator to fabricate Si-based FGTs. The LNO layer serves as a useful metal oxide bottom electrode and at the same time forms a template to promote the *a*-axis preferential orientation growth of BNT films. In the study, ZnO thin films are chosen as the channel layer of FGTs because of its low cost, low photosensitivity, and high mobility.<sup>20</sup> On the other hand, pulsed laser deposition (PLD) is a unique technique to deposit oxide thin films and multi-layered thin films. The physical properties of oxide thin films can be easily tuned by changing the experimental conditions of PLD, such as oxygen pressure.<sup>21</sup> Meanwhile, a very clean and smooth interface can be obtained by PLD, which is specially unique to deposit oxide multi-layered thin films or devices. Therefore, PLD is chosen to deposit ZnO/BNT/LaNiO<sub>3</sub> FGTs in this study.

## Experimental

The schematic illustration of ZnO/BNT/LNO/Si FGT is shown in Fig. 1. The ZnO and BNT thin films were deposited by using a pulsed laser deposition system (PLD-5000) with KrF excimer laser (COHERENT COMPLEX 205,  $\lambda = 248$  nm, 20 ns pulse duration) at a substrate temperature of 400 and 700 °C, oxygen partial pressure of 10 and 200 mTorr, respectively.<sup>22</sup> Prior to the deposition of the BNT thin films, a 50 nm thick high (110)-oriented LNO buffer/bottom electrode layer was deposited on 6° miscut Si (100) substrate by PLD. The thickness of ZnO and BNT layers is 60 and 550 nm, respectively. Source/drain Pt electrodes were deposited on the ZnO layers using the mask

plates. The channel width (*W*) and length (*L*) of FGTs are 1500 and 200  $\mu\text{m}$ , respectively. The structures of the films were characterized by X-ray diffraction (XRD) with  $\text{Cu } K_\alpha$  radiation. The atomic force microscope (AFM) (Q-Scope 850) was used to characterize the surface roughness of the films. The polarization-electric field (*P-E*) hysteresis loops of BNT films were measured using a RT Precision Workstation ferroelectric analyzer. Transistor characteristics were measured using a semiconductor device analyzer (Agilent B1500A).

## Results and discussion

Fig. 2(a) and (b) are the XRD patterns of BNT thin films deposited on different electrodes, and the XRD pattern of BNT powders is shown in Fig. 2(c) for comparison. All of the XRD patterns are indexed according to the standard powder diffraction data of BIT. It is notice that the BNT films deposited on LNO electrodes show an *a*-axis preferential crystalline orientation, while the BNT films deposited on Pt electrodes show a *c*-axis preferential crystalline orientation. In order to support the claim, the degree of preferred orientation *F* has been calculated by using the relationship proposed by Lotgering,<sup>23, 24</sup>

$$F_{(h00)} = (P_{(h00)} - P_0) / (1 - P_0), \quad (1)$$

$$P_{(h00)} = \sum I_{(h00)} / \sum I_{(hkl)}, \quad (2)$$

$$P_0 = \sum I_{(h00)}^* / \sum I_{(hkl)}^*. \quad (3)$$

Where  $\sum I_{(h00)}$  and  $\sum I_{(hkl)}$  are the summations of measured peak intensities of the (*h*00) peaks and (*hkl*) peaks, respectively.  $\sum I_{(h00)}^*$  and  $\sum I_{(hkl)}^*$  are the total measured peak intensities for all (*h*00) peaks and (*hkl*) peaks in the powder diffraction data

Cite this: DOI: 10.1039/c0xx00000x

www.rsc.org/xxxxxx

ARTICLE TYPE

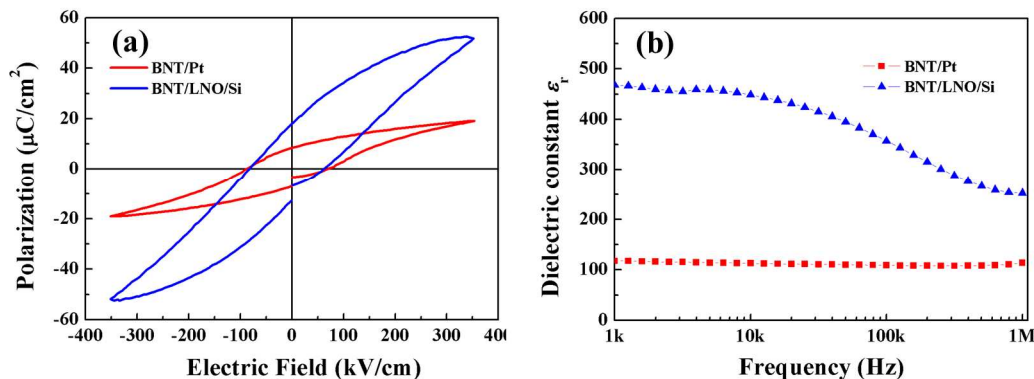


Fig. 4 (a) *P-E* hysteresis loops and (b) the frequency dependence of dielectric constant of the BNT films on different electrodes.

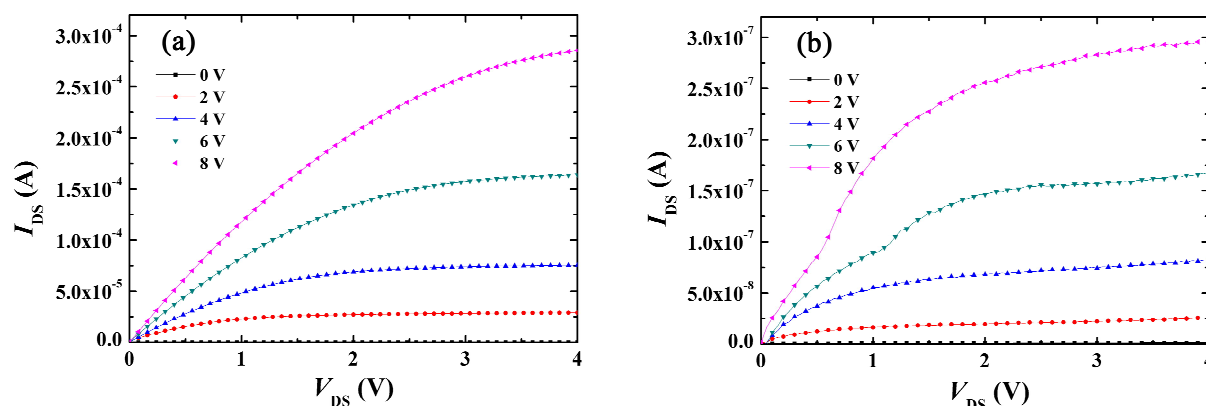


Fig. 5 Drain current and drain voltage ( $I_{DS}$ - $V_{DS}$ ) characteristics of (a) ZnO/BNT/LNO/Si and (b) ZnO/BNT/Pt FGTs.

of BNT. Therefore, the value of degree of *a*-axis-oriented of the films deposited on LNO electrodes  $F_{(h00)}$  is 32.4%, while the value of degree of *c*-axis-oriented of the films deposited on Pt electrode  $F_{(00l)}$  is 82.3% with the same method. The results demonstrate that the orientation of BNT films can be effectively modified by the LNO buffer layer.

The AFM 3D images of the BNT thin films with a scanning area of  $2 \times 2 \mu\text{m}^2$  are shown in Fig. 3. It is found that BNT thin films deposited on LNO electrodes exhibit a smoother surface morphology than the thin films on Pt electrodes. A much smaller root-mean-square roughness (RMS) of 2.156 nm for the BNT films on LNO electrodes has been obtained, which is benefit to obtain a sharp ZnO/BNT interface in the FGTs.

Fig. 4(a) and (b) show the *P-E* hysteresis loops and dielectric constant  $\epsilon_r$  as a function of frequency for the BNT thin films deposited on different electrodes, respectively. One can note that the thin films exhibit typical ferroelectric hysteresis loops on the condition of 10 kHz frequency. It is very clear that

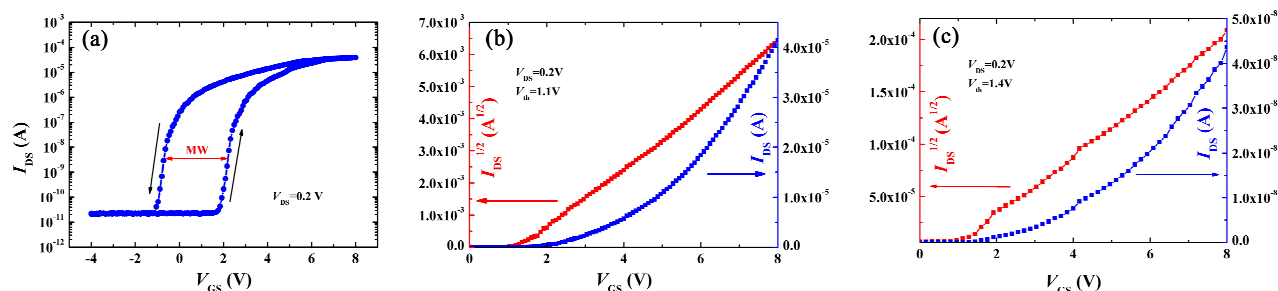
the ferroelectric polarization and dielectric constant of the BNT film are strongly dependent on the film orientation. The  $2P_r$  of the *a*-axis preferential film on LNO electrode is much larger than that of the *c*-axis preferential film on Pt electrode. The dielectric constant  $\epsilon_r = 248$  at 1 MHz of the *a*-axis preferential film is more than twice as much that  $\epsilon_r = 107$  at 1 MHz of the *c*-axis preferential film. A similar observation has been reported for BNT films prepared by using CSD method.<sup>16</sup>

Fig. 5(a) and (b) show the drain current-drain voltage ( $I_{DS}$ - $V_{DS}$ ) output characteristics of ZnO/BNT/LNO/Si and ZnO/BNT/Pt FGTs at positive gate bias from 0 to 8 V, respectively. Both of transistors show the typical *n*-channel behavior operating in enhancement mode and clear current saturation at low drain voltage. While ZnO/BNT/LNO/Si FGTs have much larger “on” current than ZnO/BNT/Pt FGTs. A large “on” current ( $2.5 \times 10^{-4}$  A) of ZnO/BNT/LNO/Si FGTs is observed when the gate voltage  $V_{GS} = 8$  V and  $V_{DS} = 4$  V, which

Cite this: DOI: 10.1039/c0xx00000x

www.rsc.org/xxxxxx

ARTICLE TYPE



**Fig. 6** (a) Drain current and drain voltage ( $I_{DS}$ - $V_{GS}$ ) logarithmic transfer characteristics of ZnO/BNT/LNO/Si FGTs. And the linear transfer characteristics including  $I_{DS}$ - $V_{GS}$  and  $I_{DS}^{1/2}$ - $V_{GS}$  curves for (b) ZnO/BNT/LNO/Si FGTs and (c) ZnO/BNT/Pt FGTs.

is larger than that of ZnO/BNT/Pt FGTs ( $2.9 \times 10^{-7}$  A).

Fig. 6(a) shows the  $I_{DS}$ - $V_{GS}$  logarithmic transfer curve of the fabricated ZnO/BNT/LNO/Si FGTs in a double sweep mode when gate voltage sweeps from -4 to 8 V at a  $V_{DS}$  of 0.2 V. A counterclockwise hysteresis loop as indicated by arrows is obtained owing to the ferroelectric polarization reversal of the BNT thin films from the  $I_{DS}$ - $V_{GS}$  characteristics curve, which shows the fabricated device has a good nonvolatile memory function. The obtained memory window (MW) and drain-current on/off ratio are as large as about 3.0 V and  $1.8 \times 10^6$ , respectively. Moreover, a low subthreshold voltage swing of 240 mV/decade is obtained.

The linear transfer characteristics  $I_{DS}$ - $V_{GS}$  and the linear fit of  $I_{DS}^{1/2}$ - $V_{GS}$  for the ZnO/BNT/LNO/Si and ZnO/BNT/Pt FGTs are shown in Fig. 6(b) and 6(c). The threshold voltage ( $V_{th}$ ) of the ZnO/BNT/LNO/Si is determined to be  $V_{th} = 1.1$  V by the  $I_{DS}^{1/2}$ - $V_{GS}$  curve of the transistors operating in the saturation region, which is slightly lower than the one ( $V_{th} = 1.4$  V) of the ZnO/BNT/Pt FGTs. The channel mobility ( $\mu_{sat}$ ) can be deduced using the equation in the saturation region for a field effect transistor,

$$I_{DS} = \left( \frac{\epsilon_0 \epsilon_r \mu_{sat} W}{2L t_{int}} \right) (V_{GS} - V_{th})^2, \quad (4)$$

where  $\epsilon_r$  is the relative permittivity at 1 MHz which we can obtain from Fig. 4(b) and  $t_{ins}$  is the thickness of BNT thin film. The  $\mu_{sat}$  of the ZnO/BNT/LNO/Si is calculated to be  $0.82 \text{ cm}^2 \text{V}^{-1} \text{s}^{-1}$ .

From the above results, one can see that the fabricated ZnO/BNT/LNO/Si FGTs have good electrical properties, such as large "on" current and low operating voltage. This can be explained as follows. On the one hand, *a*-axis preferential orientation BNT thin film obtained by using LNO buffer layer results in larger polarization and dielectric constant and thus increases the coupling of the gate electric field to the channel layer, which is very beneficial to the improvement of FGTs properties.<sup>25, 26</sup> On the other hand, it may be attributed to the relatively good interface properties between ZnO and BNT thin films owing to the smoother surface of BNT thin films on LNO

buffer layer.<sup>27, 28</sup>

## Conclusions

In summary, the Si-based FGTs with BNT as gate dielectrics and ZnO as channel layer were fabricated and characterized. The *a*-axis preferential orientation BNT gate film with a smoother surface and a significant enhancement of the polarization and dielectric constant is obtained by using LNO buffer/electrode layer. ZnO/BNT/LNO/Si transistors demonstrate good operating characteristics with a large "on" current and a low threshold voltage. The subthreshold slope, memory window, and on/off ratio are measured to be 240 mV/decade, 3.0 V and  $1.8 \times 10^6$ , respectively. The good transistor performances suggest that ZnO/BNT/LNO/Si structures are well suited for FGT application.

## Acknowledgements

This work was supported by the National Natural Science Foundation of China (Nos. 11372266, 11272274 and 11032010), the Hunan Provincial Natural Science Foundation of China (No. 12JJ1007), the Specialized Research Fund for the Doctoral Program of Higher Education (No. 20114301110004) and the Foundation for the Author of National Excellent Doctoral Dissertation of PR China (201143).

## Notes and references

- <sup>a</sup> School of Materials Science and Engineering, Xiangtan University, Hunan Xiangtan 411105, China; E-mail: xlzhong@xtu.edu.cn and jbwang@xtu.edu.cn.
- <sup>b</sup> National-Provincial Laboratory of Special Function Thin Film Materials, Xiangtan University, Hunan Xiangtan 411105, China
- L. Liang, T. Fukushima, K. Nakamura, S. Uemura, T. Kamata and N. Kobayashi, *J. Mater. Chem. C*, 2014, **2**, 879-883.
- X. Hou, Y. Xia, S. C. Ng, J. Zhang and J. S. Chang, *RSC Adv.*, 2014, **4**, 37687-37690.
- Y. Kim, L. S. O'Neil, M. Kathaperumal, L. R. Johnstone, M.-J. Pan and J. W. Perry, *RSC Adv.*, 2014, **4**, 19668-19673.
- M. Li, I. Katsouras, C. Piliago, G. Glasser, I. Lieberwirth, P. W. Blom and D. M. de Leeuw, *J. Mater. Chem. C*, 2013, **1**, 7695-7702.
- T. T. Phan, T. Miyasako, K. Higashimine, E. Tokumitsu and T. Shimoda, *Appl. Phys. A*, 2013, **113**, 333-338.

6. P. K. Nayak, J. Caraveo-Frescas, U. S. Bhansali and H. Alshareef, *Appl. Phys. Lett.*, 2012, **100**, 253507.
7. H. J. Song, P. P. Liu, X. L. Zhong, B. Li, T. Chen, F. Wang, J. B. Wang and Y. C. Zhou, *Appl. Phys. Lett.*, 2014, **105**, 053506.
- 5 8. P. Tue, T. Miyasako, E. Tokumitsu and T. Shimoda, *Adv. Mater. Sci. Eng.*, 2013, **2013**.
9. Y. Kaneko, H. Tanaka, M. Ueda, Y. Kato and E. Fujii, *IEEE T. Electron. Dev.*, 2011, **58**, 1311-1318.
10. T. Miyasako, B. N. Q. Trinh, M. Onoue, T. Kaneda, P. T. Tue, E. Tokumitsu and T. Shimoda, *Appl. Phys. Lett.*, 2010, **97**, 173509.
- 10 11. T. Fukushima, T. Yoshimura, K. Masuko, K. Maeda, A. Ashida and N. Fujimura, *Thin Solid Films*, 2010, **518**, 3026-3029.
12. D. Ito, N. Fujimura, T. Yoshimura and T. Ito, *J. Appl. Phys.*, 2003, **93**, 5563.
- 15 13. Y. Ishibashi, in *Ferroelectric Thin Films*, eds. M. Okuyama and Y. Ishibashi, Springer, 2005, pp. 3-23.
14. X. J. Lou, H. J. Zhang, Z. D. Luo, F. P. Zhang, Y. Liu, Q. D. Liu, A. P. Fang, B. Dkhil, M. Zhang, X. B. Ren and H. L. He, *Appl. Phys. Lett.*, 2014, **105**, 102907.
- 20 15. J. B. Wang, P. J. Li and X. L. Zhong, *Appl. Surf. Sci.*, 2011, **257**, 4171-4174.
16. C. Lu, Y. Qiao, Y. Qi, X. Chen and J. Zhu, *Appl. Phys. Lett.*, 2005, **87**, 222901-222901-222903.
17. H. N. Lee, D. Hesse, N. Zakharov and U. Gösele, *Science*, 2002, **296**, 2006-2009.
- 25 18. H. N. Lee, D. Hesse, N. Zakharov, S. K. Lee and U. Gosele, *J. Appl. Phys.*, 2003, **93**, 5592-5601.
19. M. Jain, B. Kang and Q. Jia, *Appl. Phys. Lett.*, 2006, **89**, 242903-242903-242903.
- 30 20. H. Dong, Y. Yang and G. Yang, *ACS Appl. Mat. Inter.*, 2014, **6**, 3093-3098.
21. Q. K. Li, J. B. Wang, B. Li, X. L. Zhong, F. Wang and C. B. Tan, *Appl. Surf. Sci.*, 2013, **283**, 623-628.
22. S. Yuan, J. Wang, X. Zhong, J. Huang and Y. Zhou, *RSC Adv.*, 2013, **3**, 24362-24366.
- 35 23. F. Lotgering, *J. Inorg. Nucl. Chem.*, 1959, **9**, 113-123.
24. G. Mambrini, E. Leite, M. Escote, A. Chiquito, E. Longo, J. Varela and R. Jardim, *J. Appl. Phys.*, 2007, **102**, 043708-043708-043706.
25. H. Sakai, H.-J. Cheong, T. Kodzasa, H. Tokuhisa, K. Tokoro, M. Yoshida, T. Ikoga, K. Nakamura, N. Kobayashi and S. Uemura, *Jpn. J. Appl. Phys.*, 2014, **53**, 05HB13.
- 40 26. H. J. Song, D. Lv, J. B. Wang, B. Li, X. L. Zhong, L. H. Jia and F. Wang, *RSC Adv.*, 2014, **4**, 54924-54927.
27. P. Schwinkendorf, M. Lorenz, H. Hochmuth, Z. Zhang and M. Grundmann, *Phys. Status Solidi A*, 2014, **211**, 166-172.
- 45 28. P. V. Thanh, B. N. Q. Trinh, T. Miyasako, P. T. Tue, E. Tokumitsu and T. Shimoda, *Ferroelectrics Lett.*, 2013, **40**, 17-29.